

The Quartz Crystal Microbalance with Dissipation Monitoring (QCM-D) Technique Applied to the Study of Membrane-Active Peptides

Torsten John,^{A,B,C} Bernd Abel,^B and Lisandra L. Martin^A

^ASchool of Chemistry, Monash University, Clayton, Vic. 3800, Australia.

^BLeibniz Institute of Surface Engineering (IOM), and Wilhelm-Ostwald-Institute for Physical and Theoretical Chemistry, Leipzig University, 04318 Leipzig, Germany.

^CCorresponding author. Email: torsten.john.research@gmail.com

Manuscript received: 28 March 2018.

Manuscript accepted: 17 May 2018.

Published online: 15 June 2018.



Torsten John received his M.Sc. degree in chemistry from Leipzig University (Germany) in 2015. He is now working under the guidance of Associate Professor Lisa Martin at Monash University and Professor Bernd Abel at Leipzig University and at the Leibniz Institute of Surface Engineering (IOM), where he is studying the aggregation of amyloidogenic and antimicrobial peptides at interfaces. Torsten John is the recipient of a 2018 Endeavour Research Fellowship.

Introduction

The quartz crystal microbalance with dissipation monitoring (QCM-D) technique is a label-free and highly sensitive approach to study binding events at a sensor surface in real-time.^[1–5] QCM-D is based on the piezoelectric effect where the fundamental frequency of the oscillating quartz sensor is dependent on its mass.^[6–8] Mass binding to the sensor surface thus causes a measurable frequency decrease ($\Delta m \propto -\Delta f$). The QCM-D technique also enables the measurement of the viscoelasticity and spatial distribution of an adlayer on the sensor surface.^[9,10]

QCM-D was traditionally used for thin and dried surfaces;^[11] however, its use has recently become popular to study biological materials in solution, such as peptide-membrane interactions.^[4] Biological membranes are mimicked by artificial lipid bilayers, that can be deposited onto gold^[12–14] or silicon^[15] coated quartz sensors. In the case of gold-coated sensors, a self-assembled monolayer of thiols is deposited before the lipid deposition to encourage a complete bilayer formation (see Fig. 1a).^[3,14,16] Various membrane types are reproduced using their major lipid

components.^[17] This enables the study of mammalian membranes, containing cholesterol,^[12,16] or bacterial membranes with anionic character,^[18,19] for example. The lipid mixtures are sonicated or extruded to obtain unilamellar liposomes before deposition onto the quartz crystal sensors.^[3,14] The peptide of interest can be introduced into the system and its interaction with the membrane is revealed through changes in frequency and dissipation of the lipid coated quartz sensor.^[1,16,20,21]

The temporal changes in frequency (Δf) and dissipation (ΔD) over the course of a typical QCM-D experiment are presented in Fig. 1b. Each QCM-D experiment starts in the buffer of choice, followed by the deposition of liposomes. The liposomes bind to the sensor surface and are ruptured either spontaneously, or by using a buffer with a lower salt concentration due to osmotic pressure to form a lipid bilayer. After the successful deposition of the lipid bilayer, the membrane layer is stabilised in buffer before the peptide of interest is introduced to study its membrane effect. The experimental details have been previously published.^[16,18,21]

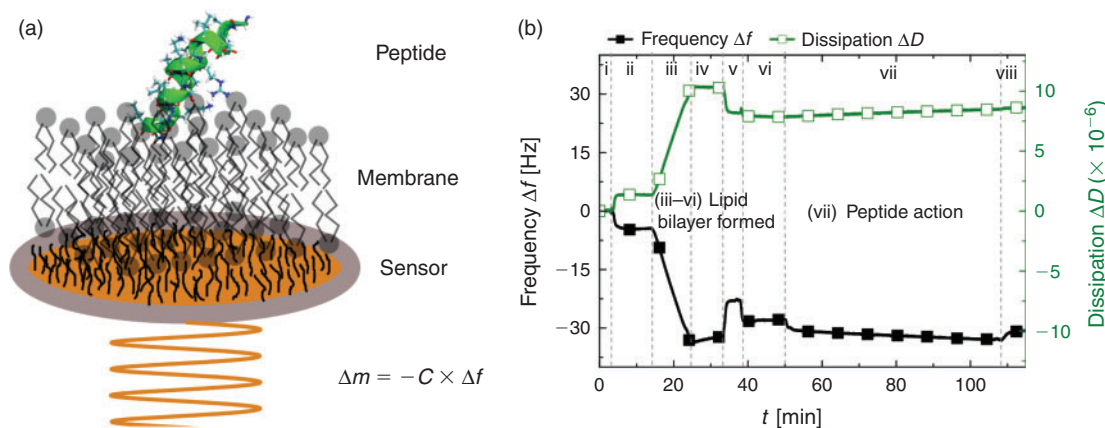


Fig. 1. (a) Schematic representation of the QCM-D experiment with a gold-coated quartz crystal sensor, deposited lipid bilayer (membrane), and the peptide of interest. The fundamental relationship between the change in mass (Δm) and change in frequency (Δf) of the oscillating quartz crystal is described by the Sauerbrey equation ($\Delta m = -C \times \Delta f$ where C is the mass sensitivity constant).^[17] (b) Δf and ΔD traces versus time of a typical QCM-D experiment with (i) water baseline, (ii) buffer baseline, (iii) liposome deposition, (iv) buffer wash, (v) liposome bursting with a lower salt concentrated buffer, (vi) lipid bilayer baseline in buffer of choice, (vii) peptide action, and (viii) buffer wash. 3D representation of the peptide was visualised using the *VMD 1.9.3* software package.^[22] (Fig. 1a is adapted from John et al. 2017.^[16])

Applications and Discussion

Biological membranes can be unaltered, distorted, or disrupted upon interaction with biomolecules, such as peptides or proteins.^[13,18,23,24] Antimicrobial peptides (AMPs) typically disrupt bacterial membranes, although pore formation or transient passage can also occur.^[13,18,25] The antimicrobial peptide uperin 3.5^[26,27] has recently been found to show membrane activity but also amyloidogenic character.^[13,28] QCM-D was used to study the peptide interaction with various model membranes (see Fig. 2).^[13] The uperin 3.5 wild-type peptide disrupts the eukaryotic and bacterial (squares in Fig. 2), but binds to the mammalian membrane models (circles in Fig. 2). As an example for a carpet-like membrane disruption, the temporal changes in frequency $\Delta f(t)$ and dissipation $\Delta D(t)$ for the cell-penetrating peptide TAT (49–57) in interaction with a bacterial membrane model are shown (triangles in Fig. 2).^[3,23] An increase in frequency relates to a loss of mass and membrane disruption, whereas a decrease in frequency is related to mass binding to the lipid bilayer. The dissipation values account for the viscoelasticity of the adlayer. An increase in dissipation is associated with a softer adlayer structure, whereas a decrease in dissipation suggests a stiffening of the adlayer. Small changes in dissipation indicate small structural rearrangements, whereas large changes in dissipation suggest significant structural rearrangements, such as the removal of the lipid bilayer.

The temporal component of the QCM-D data can be removed and a characteristic ‘fingerprint’ representation is obtained, in which the change in dissipation ΔD

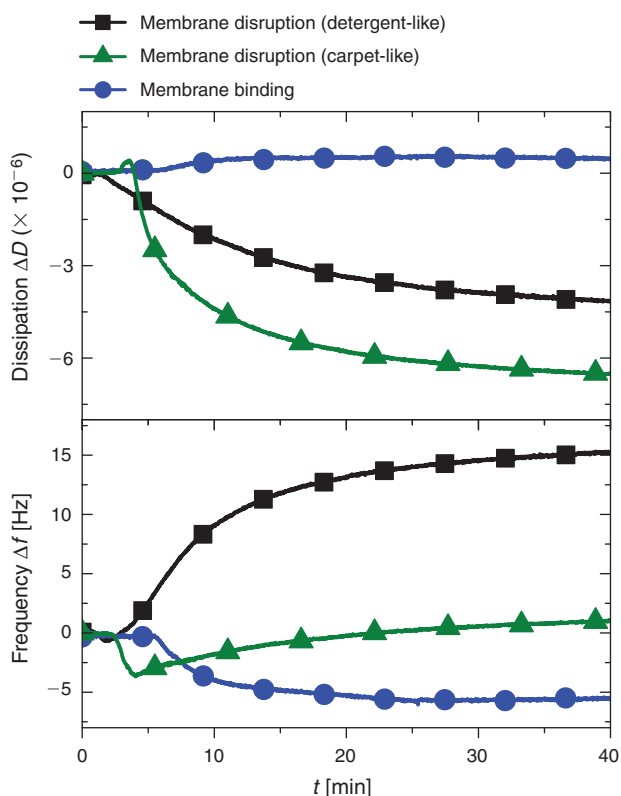


Fig. 2. Typical $\Delta f(t)$ and $\Delta D(t)$ data for peptide–membrane disruption (squares and triangles) and peptide–membrane binding (circles). The data presented are exemplary for possible peptide–membrane interaction mechanisms and taken from previous studies.^[3,13,23] Squares: interaction of 25 μM uperin 3.5 wild-type peptide with pure DMPC (eukaryotic membrane model),^[13] triangles: interaction of 10 μM TAT (49–57) peptide with 4 : 1 (v/v) DMPC/DMPG (bacterial membrane model)^[3,23] and circles: interaction of 25 μM uperin 3.5 wild-type peptide with $x_i = 30\%$ cholesterol-containing DMPC (mammalian membrane model)^[13] lipid bilayers. Data for the 7th harmonic are shown (DMPC: 1,2-dimyristoyl-*sn*-glycero-3-phosphocholine, DMPG: 1,2-dimyristoyl-*sn*-glycero-3-phospho-(1'-*rac*-glycerol)).

(viscoelasticity) is plotted versus the change in frequency Δf (mass) (see Fig. 3), revealing the structural organisation of the lipid bilayer. The bottom left quadrant (positive Δf , negative ΔD) is characteristic for mass loss and thus membrane disruption, whereas the top right quadrant (negative Δf , positive ΔD) is characteristic for membrane binding.^[13,16] Mass binding combined with a decrease in dissipation (negative Δf , negative ΔD , bottom right quadrant) indicates structural changes and rearrangements in the lipid bilayer, such as the transmembrane insertion of peptides while making the bilayer structure more rigid.^[2,18] Data in the top left quadrant are uncommon for peptide–membrane interactions because immediate mass (lipid) loss (positive Δf) usually leads to a more rigid (negative ΔD), not softer (positive ΔD), adlayer structure.

To probe the influence of the peptide on the membrane structure, at several distances from the sensor surface, the harmonics of the quartz crystal’s fundamental frequency can be obtained (see Fig. 4). Higher harmonics probe the membrane layer closer to the gold sensor surface, whereas lower harmonics probe interactions furthest from the sensor and even above the lipid bilayer.^[5,13,16] The spread in harmonics can be indicative of the peptide–membrane interaction mechanism; a high spread indicates surface binding or membrane disruption (Fig. 4b after 5 min) while a low spread indicates pore formation or a transmembrane insertion (Fig. 4a and b, until 5 min).^[3,13]

QCM-D is a nanogram sensitive technique that provides valuable information about the mode of action of biomolecules towards lipid bilayers of varying composition. The analysis of both the change in mass (frequency) and viscoelasticity (dissipation) over the range of several harmonics provides insights into the peptide–membrane action. The $\Delta f(t)$ and $\Delta D(t)$ analysis enables the elucidation of the membrane mechanism (binding versus disruption) and can distinguish between surface processes and transmembrane insertion. This facilitates a comprehensive study of membrane-active peptides. A schematic overview of peptide–membrane interaction mechanisms is presented in Fig. 5.

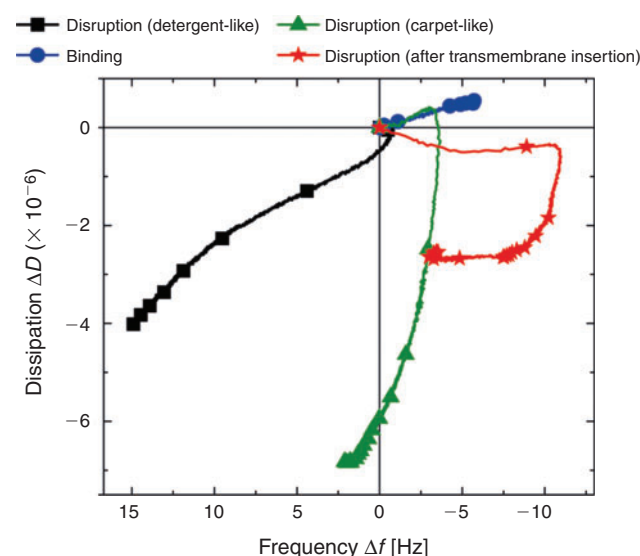


Fig. 3. Typical ΔD versus Δf plots for peptide–membrane disruption (squares, triangles, stars) and peptide–membrane binding (circles). The data presented are exemplary for possible peptide–membrane interaction mechanisms and taken from previous studies.^[2,3,13,23] Squares: interaction of 25 μM uperin 3.5 wild-type peptide with pure DMPC (eukaryotic membrane model),^[13] triangles: interaction of 10 μM TAT (49–57) peptide with 4 : 1 (v/v) DMPC/DMPG (bacterial membrane model),^[3,23] circles: interaction of 25 μM uperin 3.5 wild-type peptide with $x_i = 30\%$ cholesterol-containing DMPC (mammalian membrane model) and stars: interaction of 20 μM melittin peptide with pure DMPC (eukaryotic membrane model) lipid bilayers. Data for the 7th harmonic are shown. The point of origin (0,0) corresponds to the time of peptide addition. (The dataset for melittin was kindly provided by Dr Stefania Piantavigna.)

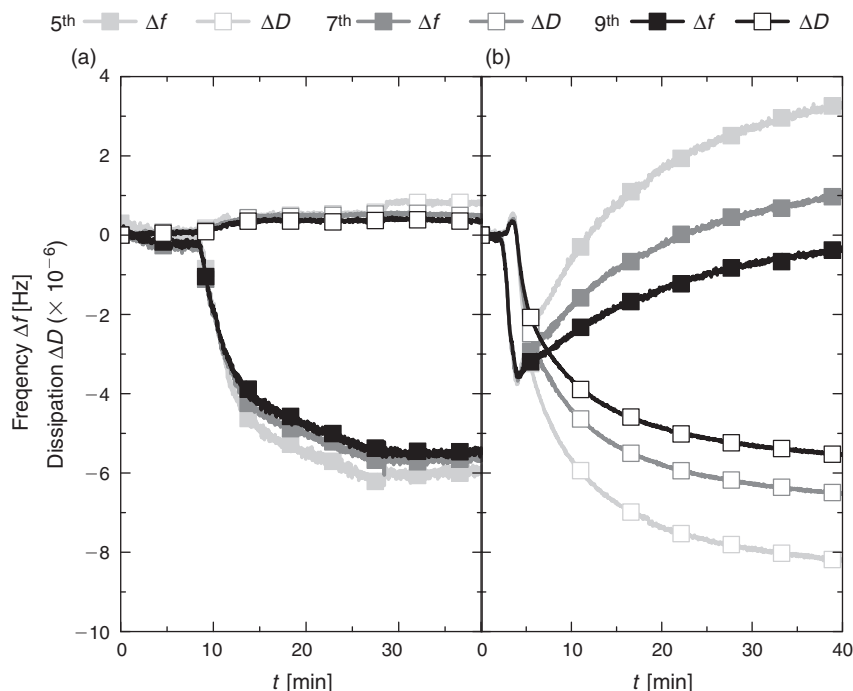


Fig. 4. Typical Δf and ΔD plots versus time showing the response for the different harmonics (5th, 7th, and 9th) for (a) transmembrane binding (pore-like) and (b) carpet-like disruption. The data presented are exemplary for possible peptide–membrane interaction mechanisms and taken from previous studies.^[3,13,23] (a) Interaction of 25 μM uperin 3.5 wild-type peptide with pure DMPC lipid bilayers (eukaryotic membrane mode) and (b) interaction of 10 μM TAT (49–57) peptide with 4 : 1 (v/v) DMPC/DMPG lipid bilayers (bacterial membrane model).^[3,23]

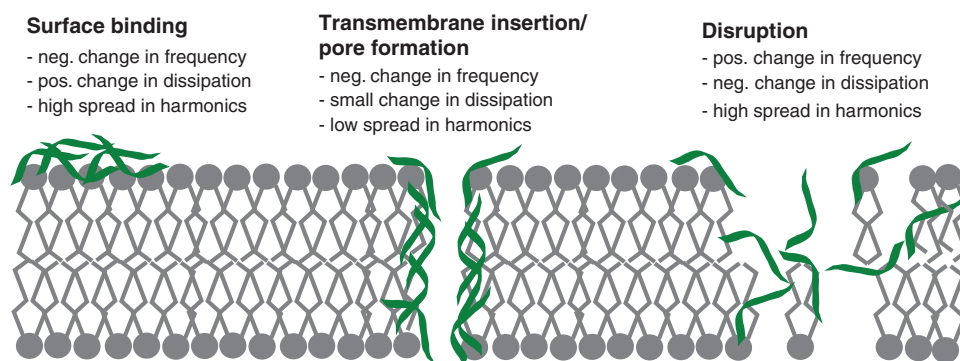


Fig. 5. Overview of peptide–membrane interaction mechanisms that can be probed and distinguished using the QCM-D technique. Peptide–membrane surface binding leads to a mass increase (negative Δf) and increase in viscoelasticity (positive ΔD) of the adlayer, predominately for the harmonics that probe distances far away from the sensor surface (spread in harmonics). Transmembrane peptide insertion and pore formation lead to a mass increase (negative Δf) for all harmonics (low spread) and small changes in dissipation (ΔD). Membrane disruption is visible by a significant mass decrease (positive Δf) and decrease in dissipation (negative ΔD) which is mostly detected for distances far from the sensor surface (high spread in harmonics).

Conflicts of interest

The authors declare no conflicts of interest.

Acknowledgements

This work was supported by the German Science Foundation (DFG, SFB-TRR 102, project B1). TJ thanks the Friedrich-Ebert-Stiftung for a PhD fellowship, and the Australian Government Department of Education and Training and Scope Global for the support through a 2018 Endeavour Research Fellowship.

References

[1] A. Mechler, S. Praporski, K. Atmuri, M. Boland, F. Separovic, L. L. Martin, *Biophys. J.* **2007**, *93*, 3907. doi:10.1529/BIOPHYSJ.107.116525
 [2] G. A. McCubbin, S. Praporski, S. Piantavigna, D. Knappe, R. Hoffmann, J. H. Bowie, F. Separovic, L. L. Martin, *Eur. Biophys. J.* **2011**, *40*, 437. doi:10.1007/S00249-010-0652-5
 [3] S. Piantavigna, G. A. McCubbin, S. Boehnke, B. Graham, L. Spiccia, L. L. Martin, *Biochim. Biophys. Acta, Biomembr.* **2011**, *1808*, 1811. doi:10.1016/J.BBAMEM.2011.03.002
 [4] A. Janshoff, H.-J. Galla, C. Steinem, *Angew. Chem. Int. Ed.* **2000**, *39*, 4004. doi:10.1002/1521-3773(20001117)39:22<4004::AID-ANIE4004>3.0.CO;2-2
 [5] K. F. Wang, R. Nagarajan, C. M. Mello, T. A. Camesano, *J. Phys. Chem. B* **2011**, *115*, 15228. doi:10.1021/JP209658Y
 [6] C. Fredriksson, S. Kihlman, M. Rodahl, B. Kasemo, *Langmuir* **1998**, *14*, 248. doi:10.1021/LA971005L
 [7] G. Sauerbrey, *Z. Phys.* **1959**, *155*, 206. doi:10.1007/BF01337937
 [8] M. C. Dixon, *J. Biomol. Tech.* **2008**, *19*, 151.
 [9] M. Rodahl, F. Höök, C. Fredriksson, C. A. Keller, A. Krozer, P. Brzezinski, M. Voinova, B. Kasemo, *Faraday Discuss.* **1997**, *107*, 229. doi:10.1039/A703137H

- [10] N.-J. Cho, K. K. Kanazawa, J. S. Glenn, C. W. Frank, *Anal. Chem.* **2007**, *79*, 7027. doi:10.1021/AC0709504
- [11] B. Kasemo, E. Tornqvist, *Phys. Rev. Lett.* **1980**, *44*, 1555. doi:10.1103/PHYSREVLETT.44.1555
- [12] S. E. Stewart, C. H. Bird, R. F. Tabor, M. E. D'Angelo, S. Piantavigna, J. C. Whisstock, J. A. Trapani, L. L. Martin, P. H. Bird, *J. Biol. Chem.* **2015**, *290*, 31101. doi:10.1074/JBC.M115.683078
- [13] L. L. Martin, C. Kubeil, S. Piantavigna, T. Tikkoo, N. P. Gray, T. John, A. N. Calabrese, Y. Liu, Y. Hong, M. A. Hossain, N. Patil, B. Abel, R. Hoffmann, J. H. Bowie, J. A. Carver, *Pept. Sci.* **2018**, *110*, e24052. doi:10.1002/PEP2.24052
- [14] A. Mechler, S. Praporski, S. Piantavigna, S. M. Heaton, K. N. Hall, M.-I. Aguilar, L. L. Martin, *Biomaterials* **2009**, *30*, 682. doi:10.1016/J.BIOMATERIALS.2008.10.016
- [15] C. A. Keller, B. Kasemo, *Biophys. J.* **1998**, *75*, 1397. doi:10.1016/S0006-3495(98)74057-3
- [16] T. John, Z. X. Voo, C. Kubeil, B. Abel, B. Graham, L. Spiccia, L. L. Martin, *MedChemComm* **2017**, *8*, 1112. doi:10.1039/C7MD00054E
- [17] H. Kamimori, K. Hall, D. J. Craik, M. I. Aguilar, *Anal. Biochem.* **2005**, *337*, 149. doi:10.1016/J.AB.2004.10.028
- [18] S. Praporski, A. Mechler, F. Separovic, L. L. Martin, *ChemPlusChem* **2015**, *80*, 91. doi:10.1002/CPLU.201402318
- [19] D. Knappe, S. Piantavigna, A. Hansen, A. Mechler, A. Binas, O. Nolte, L. L. Martin, R. Hoffmann, *J. Med. Chem.* **2010**, *53*, 5240. doi:10.1021/JM100378B
- [20] K. A. Marx, *Biomacromolecules* **2003**, *4*, 1099. doi:10.1021/BM020116I
- [21] C. Kubeil, J. C. I. Yeung, R. C. Tuckey, R. J. Rodgers, L. L. Martin, *ChemPlusChem* **2016**, *81*, 995. doi:10.1002/CPLU.201600272
- [22] W. Humphrey, A. Dalke, K. Schulten, *J. Mol. Graph.* **1996**, *14*, 33. doi:10.1016/0263-7855(96)00018-5
- [23] S. Piantavigna, M. E. Abdelhamid, C. Zhao, X. Qu, G. A. McCubbin, B. Graham, L. Spiccia, A. P. O'Mullane, L. L. Martin, *ChemPlusChem* **2015**, *80*, 83. doi:10.1002/CPLU.201402209
- [24] S. E. Stewart, M. E. D'Angelo, S. Piantavigna, R. F. Tabor, L. L. Martin, P. I. Bird, *Biochim. Biophys. Acta, Biomembr.* **2015**, *1848*, 115. doi:10.1016/J.BBAMEM.2014.10.012
- [25] Y. Shai, *Biochim. Biophys. Acta, Biomembr.* **1999**, *1462*, 55. doi:10.1016/S0005-2736(99)00200-X
- [26] J. H. Bowie, F. Separovic, M. J. Tyler, *Peptides* **2012**, *37*, 174. doi:10.1016/J.PEPTIDES.2012.06.017
- [27] A. M. Bradford, J. H. Bowie, M. J. Tyler, J. C. Wallace, *Aust. J. Chem.* **1996**, *49*, 1325. doi:10.1071/CH9961325
- [28] A. N. Calabrese, Y. Liu, T. Wang, I. F. Musgrave, T. L. Pukala, R. F. Tabor, L. L. Martin, J. A. Carver, J. H. Bowie, *ChemBioChem* **2016**, *17*, 239. doi:10.1002/CBIC.201500518